Exam: Spin model of magnetic materials

TFY4235 Computational Physics

Jostein N. Kløgetvedt, Cand. no. 10033
Department of Physics, Norwegian University of Science and Technology,
Trondheim Norway

May 1, 2022

Contents

1 Introduction **2**
1.1 Dimensionless numbers 2
1.2 Analytical solution 2

2 Implementation **3**

3 Results and Discussion **4**
3.1 Single-spin dynamics 4
3.2 Chain of spins 5
3.3 Lattice spin 10

Bibliography **13**

1 Introduction

The theoretical background is gathered from the project description [Sim]. The Hamiltonian of the system is given by

$$H = -J\sum_{\text{n.n}} \vec{S}_j \cdot \vec{S}_k - d_z \sum_{j=1}^{N} (\vec{S}_j \cdot \hat{e_z})^2 - \mu_s \sum_{j=1}^{N} \vec{S}_j \cdot \vec{B}_j, \tag{1}$$

and the equation of motion for the spins is given by the LLG equation

$$\partial_t \vec{S}_j = \frac{-\gamma}{1+\alpha^2}\left[\vec{S}_j \times \vec{F}_j + \alpha \vec{S}_j \times (\vec{S}_j \times \vec{F}_j)\right]. \tag{2}$$

The quantity $\vec{F}_j$ may be split up into two parts,

$$\vec{F}_j = -\frac{1}{\mu_s}\frac{\delta H}{\delta \vec{S}_j} + \vec{\Gamma}\sqrt{\frac{2\alpha k_b T}{\gamma \mu_s \Delta t}}, \tag{3}$$

where $\vec{\Gamma}$ are random numbers from a standard normal distribution. The functional derivative may be treated as the partial derivative. Performing the differentiation we find

$$-\frac{1}{\mu_s}\frac{\partial H}{\partial \vec{S}_j} = 2\frac{J}{\mu_s}\sum_{\text{n.n}} \vec{S}_i + 2\frac{d_z}{\mu_s} S_{j,z}\hat{e}_z + \vec{B}. \tag{4}$$

1.1 Dimensionless numbers

We may express Eq. (2) in dimensionless form. As a start, we introduce $\kappa = d_z/J$, $\beta = \mu_s B/J$ such that $\vec{\tilde{F}}_j = \vec{F}_j/\vec{B}_j$ may be written

$$\vec{\tilde{F}}_j = \frac{1}{\beta}\left[2\text{sign}(J)\sum_{\text{n.n}} \vec{S}_i + 2\kappa S_{j,z}\hat{e}_z + \vec{\beta}_j\right] + \vec{\Gamma}\sqrt{\frac{2\alpha k_b T}{\beta J \Delta \tilde{t}}}, \tag{5}$$

where we have differentiated the Hamiltonian and introduced $\tilde{t} = \gamma B t$. Differentiating Eq. (2) with the dimensionless time we find

$$\partial_{\tilde{t}} \vec{S}_j = -\frac{1}{1+\alpha^2}\left[\vec{S}_j \times \vec{\tilde{F}}_j + \alpha \vec{S}_j \times (\vec{S}_j \times \vec{\tilde{F}}_j)\right]. \tag{6}$$

1.2 Analytical solution

One may derive an analytical solution to the problem if $T = \alpha = 0$, for a single-spin. We also set $\vec{B} = 0$, but keep $d_z > 0$, so $\vec{\tilde{F}}_j$ takes the form $\vec{\tilde{F}}_j = \frac{2\kappa}{\beta} S_{j,z}\hat{e}_z$. Inserting this in Eq. (6) we find

$$\partial_{\tilde{t}} \vec{S}_j = -\frac{2\kappa}{\beta} S_{j,z}(\vec{S}_j \times \hat{e}_z) = -\frac{2\kappa}{\beta} S_{j,z}(S_{j,y}\hat{e}_x - S_{j,x}\hat{e}_y) \tag{7}$$

This implies $\partial_{\tilde{t}} S_{j,z} = 0$. The equations for the x and y component takes the form

$$\begin{aligned} \partial_{\tilde{t}}^2 S_x &= -\omega^2 S_x \\ \partial_{\tilde{t}}^2 S_y &= -\omega^2 S_y \end{aligned} \tag{8}$$

with $\omega = 2S_z\frac{\kappa}{\beta}$. The solutions are harmonic oscillators, i.e. a precession of the spin around the z-axis.

2 Implementation

We utilize Heun's method to integrate the ODE. Generally can Heun's method solve ODEs on the form $\partial_t y = f(t, y(t))$ numerically by iterating forward in time with a predictor and a corrector step. In our case will $f(t, y(t))$ equal Eq. (6) with different expressions for $\vec{F}_j$ according to what type of system we are looking at, i.e. $T = 0$ or $\alpha = 0$ yields different expressions. The spins need to be normalized such that $|\vec{S}_j(t)| = 1$. This is achieved by projecting the solution at each time step back to the unit sphere.

The implementation is written in Python and utilizes the libraries NumPy and SciPy. Moreover, the the compiler Numba are utilized in some cases where efficiency is needed. With some cases we mean that the decorator `@nb.njit` are inserted above important functions in order to reduce the computation time. The decorator translates Python functions to optimized machine code at runtime using the industry-standard LLVM compiler library.

A general Heun step-function adapted to any size of y takes the form `heun_step(y,dt,f,*args)`. We note that our $f(t, y(t))$ does not explicitly depend on t, so t is removed from the arguments in the step-function. The not yet specified arguments `*args` are passed down to a specific function `f(y,*args)` corresponding to the particular expression for $f(y(t))$ we are investigating. For instance, when we consider damping of a chain of spins will α be passed as a parameter while $T = 0$ for all cases. We note that we could have made a general function for $f(y(t))$ dealing with all the specific cases, but we find that making specific functions makes the code less error-prone and efficient.

We consider three different spin systems; single-spin, a spin chain and a spin lattice. We treat the single-spin separately since the data is structured differently. In the single-spin case is the spin at a given time-step, `S`, represented by a 1D vector with three elements containing all the components. The cross product in $f(y)$ is then calculated with `numpy.cross()` and the spin is normalized by `numpy.linalg.norm()`. For the multiple spin case are the spins at a time-step represented by a $N \times 3$ matrix, N being the number of spins. The whole matrix is inserted into the step-function and we compute the next spin configuration in a single Heun iteration. Home-made functions are used to normalize each row in the matrix, as well as taking the cross product between two matrices, row by row.

The summation over nearest neighbours is easily implemented in the spin chain case. Denoting the resulting summation at site i for `res[i]`, we may simply iterate over $i = 1, \ldots, N-2$ with the formula `res[i]=S[i-1]+S[i+1]`. The boundary values, $i = 0, N-1$, depend on whether we use periodic boundary conditions (PBC) or not. The expressions are `res[0]=S[1]+S[-1]` and `res[N-1]=S[N-2]+S[0]` with PBC, and the last two terms are excluded when considering a closed system. Now, for the spins on a lattice, the dimensions of the matrix containing all the spins is $N^2 \times 3$, when the square lattice has dimensions $N \times N$. This means that the lattice sites are mapped onto a 1D "vector" of spins with length N^2. To be more specific, a lattice site located at (j, i) (j being the row and i being the column) for $i, j = 0, 1, \ldots N-1$ is mapped to $q = jN + i, \quad q = 0, 1, \ldots, N^2 - 1.$ in the 1D vector. When performing the summation over all nearest neighbours is the mapping function $q(j, i)$ used heavily. The summation for the internal lattice sites are calculated as `res[q(j,i)]=S[q(j-1,i)+S[q(j+1,i)+S[q(j,i-1)]+S[q(j,i+1)]` for $i, j = 1, \ldots N-2$. The sites on the boundary are treated separately where the four corners are written out explicitly and the remaining boundary sites are calculated in a single for-loop.

Random numbers from the uniform and Gaussian distribution are generated with `numpy.random.uniform()` and `numpy.random.normal()` respectively. A seed is set to produce a specific random sequence, in particular the command `numpy.random.seed(42)` is used.

3 Results and Discussion

3.1 Single-spin dynamics

In the single-spin dynamics is $N = 1$, obviously, and there is no coupling term in the Hamiltonian. Moreover is $\vec{B}$ and T set equal to zero, but we keep $d_z > 0$. We then end up with the simple expression $\vec{\tilde{F}}_j = \frac{2\kappa}{\beta}\vec{S}_{j,z}\hat{e_z}$. Eq. (6) is solved with this expression for $\vec{\tilde{F}}_j$. Moreover, the used parameters are $\beta = \kappa = 0.1$ with the initial condition $\vec{S_0} = [0.04, 0.20, 0.98]^T$ (approximately). We refer to this problem as single-spin dynamics (SSD), and we solve with it for the damped, $\alpha > 0$, and undamped, $\alpha = 0$, case.

Task a). We start with the case where $\alpha = 0$ so there is no damping in the system. The ODE then simplifies to Eq. (7) where an analytical solution is known. The analytical solutions for S_x and S_y are harmonic oscillations, as derived in Section 1.2. The frequency is determined to be $\omega = \frac{2\kappa S_{j,z}}{\beta} \approx 2$ with the chosen parameters. The numerical solution of each components are shown in Fig. 1a, together with the analytical solutions, plotted as dashed lines. The solution is computed till the end-time $T_{\text{end}} = 5\omega$ on a low resolution grid, $n = 100$ points, to visibly separate the numerical from the analytical solutions. We observe a good correlation, and we may also observe that the S_z-component is constant in time, as it should.

Task b). We look now at the same problem as in a), SSD, but with $\alpha = 0.05$. There is now damping in the system. The numerical solution is shown in Fig. 1b. The plot clearly illustrates damping of the amplitudes. We may also see that S_z goes towards one to keep the spin normalized when S_x and S_y decreases.

The project description, [Sim], introduces the decay constant $\tau = \frac{1}{\alpha\omega}$. In our case, where ω depends on $S_{j,z}$ will the decay constant change over time. However, this is with a small amount, as one can observe from the plot, where $S_{j,z}$ is approximately equal to one for all times. We may therefore treat τ as a constant. Fig. 2 illustrates the damping in more detail, and show how the analytical, $\tau = 1/(\alpha\omega) = 10.21$, compares with the computed graph where $\tau = 10.23$. There is a strong compliance with the results so we may say that the prediction made by linear spin wave theory is correct when $S_{0_z} \gg S_{0_x}, S_{0_y}$. We note that the computed τ, is found by the function `scipy.optimize.curve_fit()`, where we fit an exponential function with the decay constant as parameter.

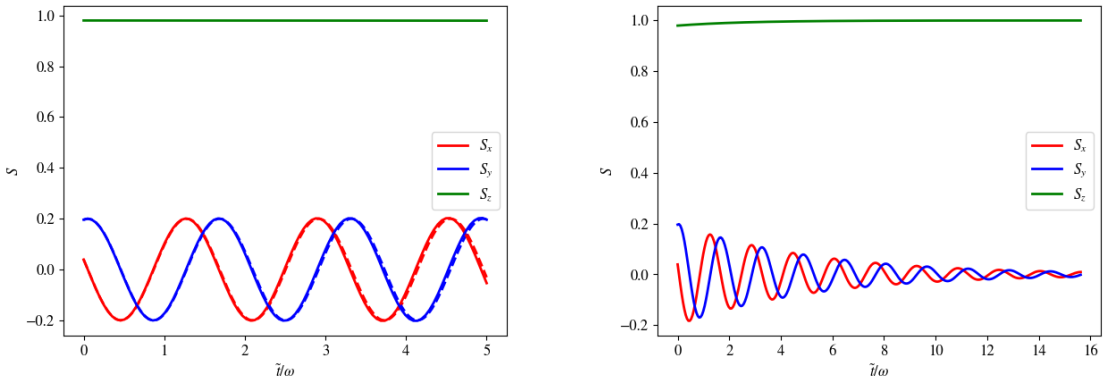

(a) No damping, $\alpha = 0$.

(b) Damping, $\alpha = 0.05$.

Figure 1: Plot of each component of the spin in the single-spin dynamic problem, SSD, for both the damped and undamped case. The numerical solution in Fig. 1b is computed with $n = 100$, and the analytical solutions are plotted as dashed lines. The numerical solution in Fig. 1b is computed with $n = 300$ due to the longer time interval.

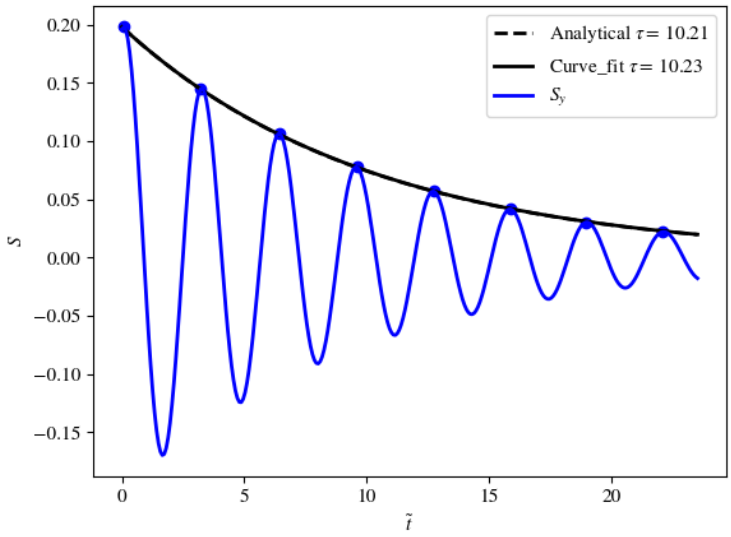

Figure 2: Numerical solution of SSD with $\alpha = 0.05$, where the S_y component is shown as a function of time. A resolution of $n = 300$ points is used. The exponential decay of the amplitude is shown for both the analytical and the computed value of the decay constant.

3.2 Chain of spins

Introducing multiple spins on a 1D chain, we will again look at the case where $\vec{B}, T = 0$ and $d_z > 0$. We then find $\vec{\tilde{F}}_j = \frac{2}{\beta}\text{sign}(J)\sum_{\text{n.n}}\vec{S}_i + \frac{2\kappa}{\beta}S_{j,z}\hat{e}_z$. We solve Eq. (6) with this expression for $\vec{\tilde{F}}_j$. The used parameters are in this case $\beta = 0.4$, $\kappa = 0.3$ and the initial configuration is such that all spins align towards $\hat{e}_z$, except for the spin at the first site which is tilted a bit. This spin is set equal to $\vec{S}_0 = [0.09, 0.0, 0.99]^T$ (approximately). We refer to this problem as spin chain dynamics (SCD), and we shall vary the parameters N and α. We start by looking at $J > 0$.

Task c). We investigate a small system where we have $N = 9$ spins with $J > 0$ and no periodic boundary conditions. Moreover is the damping constant equal to $\alpha = 0.1$. The solution is calculated with $n = 700$. Fig. 3a illustrates how the S_z and $r = \sqrt{(S_x^2 + S_y^2)} \cdot \text{sign}(S_x)$ changes with time for each spin. The $x-$component in the plot, which is r, is scaled with a constant factor to visualize the differences. We see that the excitation starting at $i = 0$ is reduced in amplitude across the chain. This is due to the damping. The end-time is chosen such that the signal, i.e. the magnon-wave, reaches the last site $i = 8$. Fig. 3b visualizes the spin in the (x, y)-plane at each site. The length of the arrows does not represent magnitude of the precession since each arrow is scaled to unity length. Here we clearly see a typical magnon precession wave, at least for the five first spins. The direction of each spin in the (x, y)-plane is rotated approximately by $\pi/4$ radians for each site. We notice that the leftmost spins are more densely packed than the ones on the other side. This is because we have no PBC so the magnon wave propagating forward does not rotate the spins that it has passed. We will come back to this in the next task. Fig. 4 shows more clearly how the magnon wave propagate through the first three lattice sites to excite S_x and S_y. We may also see how the first spins have approximately the same S_x and S_y in the time interval $0.5 < \tilde{t} < 1.4$. This is, again, due to the magnon wave being present at the opposite side of the chain.

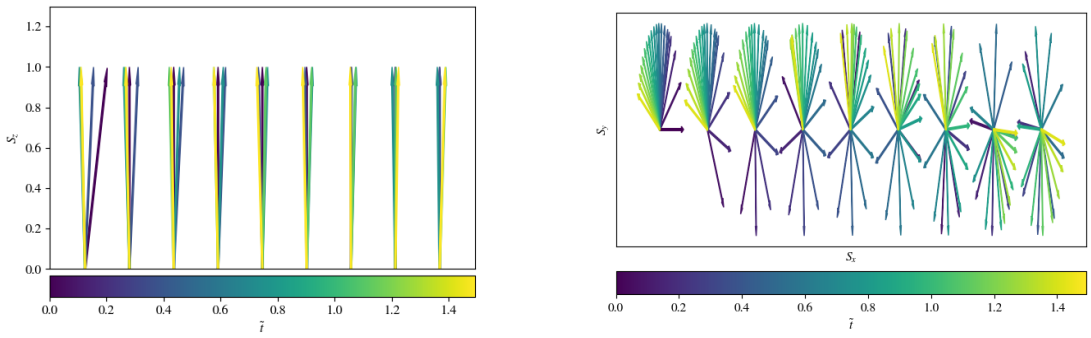

(a) (b)

Figure 3: Numerical solution to SCD with $\alpha = 0.1$ and resolution $n = 700$. The plot illustrates the precession of the spins.

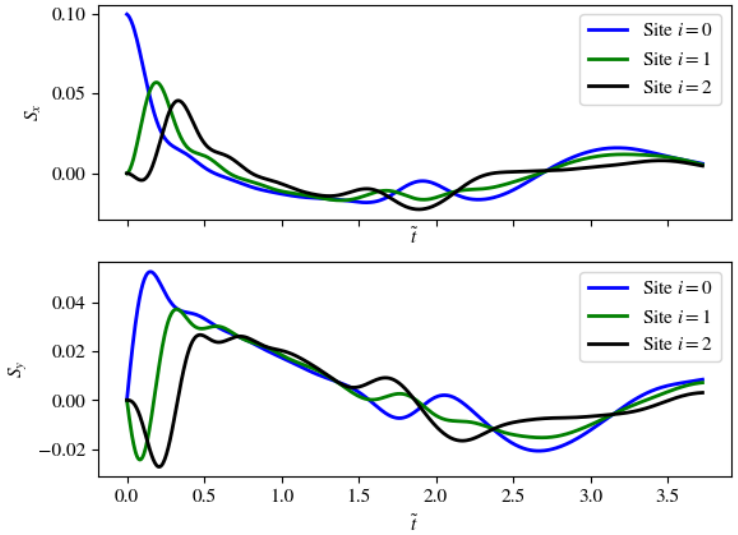

Figure 4: Numerical solution to SCD with $\alpha = 0.1$ and resolution $n = 700$. The plot shows the S_x and S_y components of the spin for the three first spins, as a function of time.

Task d). We look at the same problem as in c), but for the undamped case $\alpha = 0$. Otherwise are the same parameters used. Proceeding in a similar fashion, Fig. 5 shows the S_x and S_y components for the spins at $i = 0, 1, 8$ for the undamped case. The dynamics is similar as above, but we can here more clearly see that the system is closed, i.e. no periodic boundary conditions. The dynamics may be described as follows. Starting with the first spin, it sends a magnon wave that reaches the rightmost spin approximately at $\tilde{t} = 0.7$. This creates oscillations for the rightmost spin which then sends the wave back again. The wave comes back to start at $\tilde{t} \approx 1.4$. During the transportation time, $\tilde{t} < 1.4$, will the leftmost spins not oscillate, but slowly align with the $z-$axis due to the anisotropy constant. The system may then be described as a travelling wave going back and forth between two walls. The wave represents the amplitude of the oscillations in this case.

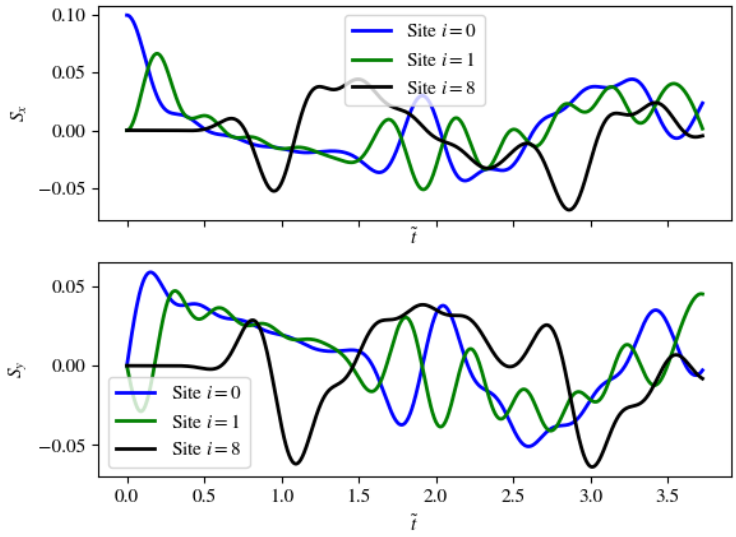

Figure 5: Numerical solution to SCD with no damping $\alpha = 0$ and resolution $n = 700$. The plot shows the S_x and S_y components of the spin for lattice points $i = 0, 1, 8$, as a function of time.

As a comparison of the damped vs. the undamped case may we take a look at Fig. 6. Here is the numerical solution, more specifically the S_x component at all lattice sites, shown with a longer chain of spins, $N = 20$. In the undamped case, as shown in Fig. 6b, can we clearly see how the wave propagates to the end on the right hand side before returning to the starting point. Once it has returned will the whole chain of spins oscillate. This is according to the discussion in the above paragraph. We may also notice that the time of return is larger than in the $N = 9$ case, this is due to the chain being longer. We see the same pattern for the damped case, only that the amplitude decreases with time. The amplitudes are decreased so much that we don't see the same sinusoidal waves in the $\tilde{t} = 3.5$ case as for the undamped. We note that we only have values of $S_{j,x}$ at each lattice site $j = 0, 1, \ldots N-1$ so interpolation is used to get a smooth curve. In particular the function `scipy.interpolate.interp1d()` is used with cubic splines.

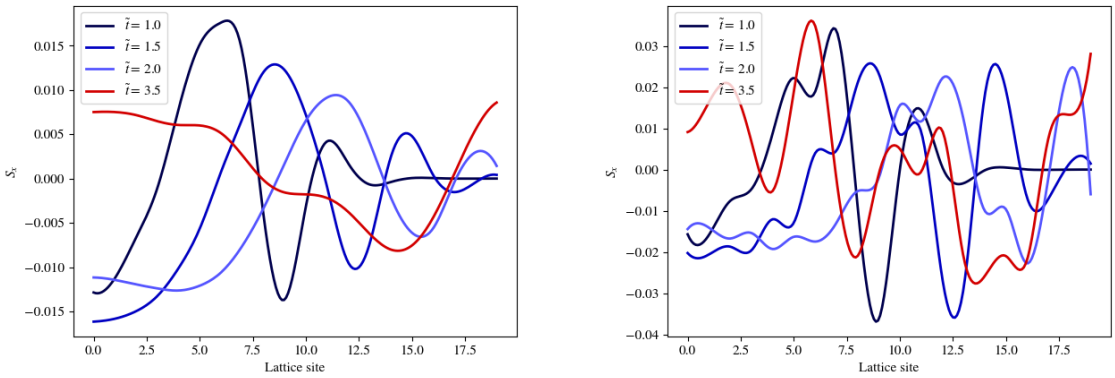

(a) No damping, $\alpha = 0$.

(b) Damping, $\alpha = 0.1$.

Figure 6: Solution to SCD with $N = 20$ and $n = 400$ for the damped and undamped cases. The plot shows S_x as a function of lattice sites. The wave of amplitudes are shown at different times.

In **Task e)**, we consider the SCD problem with $N = 9$, $\alpha = 0$ and introduce periodic boundary

conditions. The numerical solutions are shown in Fig. 7 and Fig. 8, similarly as in the previous cases. Here we note immediately a different behavior. There is no signal being transported back and forth, but rather all spins precess immediately. It might be viewed as a continuous stream of magnon waves entering the left hand side. The periodic boundary condition simulates a long, infinite, chain of spins. The solutions to this problem are then superpositions of waves propagating along the infinite chain. We see that the spins in the (x, y)-plane are not evenly distributed, especially in Fig. 7, this is due to the magnon wave is a superposition of different frequencies.

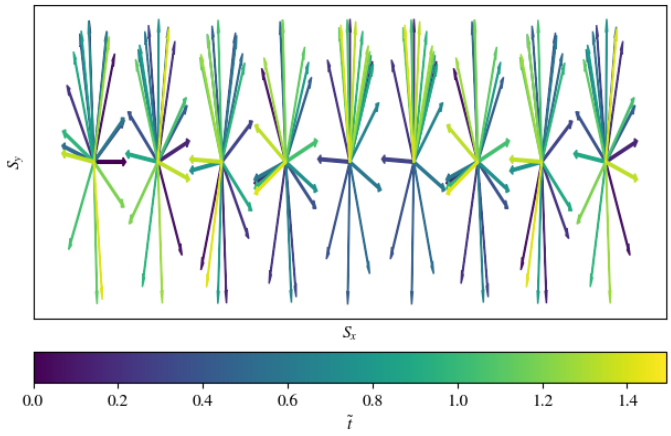

Figure 7: Numerical solution to SCD with $N = 9$, $\alpha = 0$ and we use periodic boundary conditions. The resolution is $n = 700$. The plot illustrates the precession of the spins.

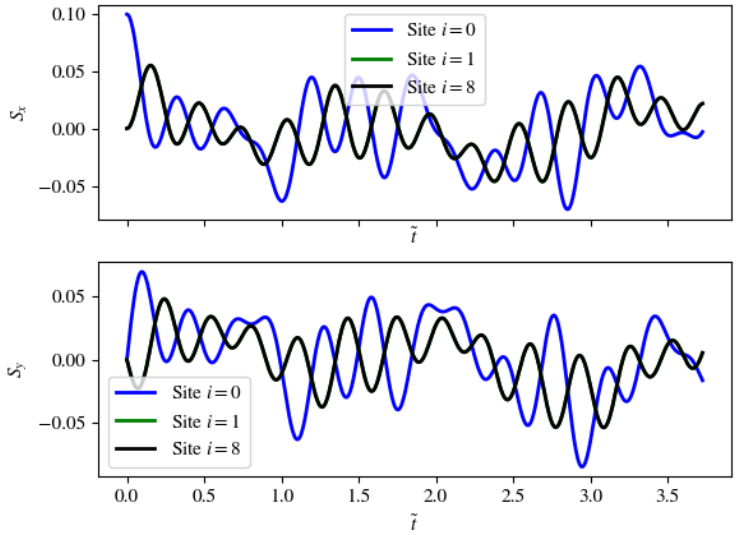

Figure 8: Numerical solution to SCD with $N = 9$, $\alpha = 0$ and we use periodic boundary conditions. The resolution is $n = 700$. The plot shows the S_x and S_y components of the spin for lattice points $i = 0, 1, 8$, as a function of time.

Task f). Considering the same problem, SCD, we solve it on a chain of $N = 20$ spins with $\alpha = 0.1$. We utilize periodic boundary conditions in this case. The initial condition is randomly configured by drawing numbers for each spin-component from a uniform distribution in the interval $[-1, 1]$. Each

spin are normalized afterwards. Since the temperature is zero, it is expected that the system will eventually end up in the semi-classical ground state. It is known that the ferromagnetic ground state corresponds to $J > 0$, and the anti-ferromagnetic has $J < 0$. Each state is characterized by having the neighbouring spin either parallel or anti-parallel to each other. The magnetization is then ± 1 or zero, if we have an even number of spins. The magnetization is the average of all the $S_{j,z}$ components. Fig. 9 shows the obtained magnetization as a function of time $\tilde{t}$. The solutions are computed till $\tilde{t}_{\text{end}} = 50$ with the resolution $n = 2500$, and are in accordance with the expected outcome. We observe that it takes longer time to settle for the FM ground state than the AFM. This might be due to the initial configuration which already has an average magnetization of approximately zero.

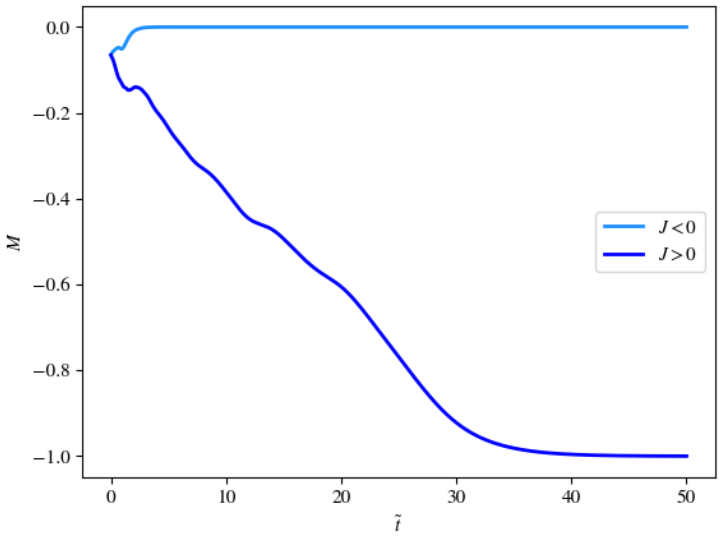

Figure 9: Magnetization as a function of time for the FM ($J > 0$) and AFM ($J < 0$) case. The numerical solution solves SCD with $N = 20$, $\alpha = 0.1$ on a grid of resolution $n = 2500$. The spins are initialized randomly, and periodic boundary conditions are utilized.

To illustrate how the spin components behave going from the disordered to ordered state, does Fig. 10 show the S_y and S_z components at each lattice site, for different times. The S_y-component for the FM case oscillates with a low frequency, its period being approximately the number of lattice sites N, while the amplitude decreases with time. The S_z-components are aligning up at $\tilde{t} \approx 37$, all pointing towards $-\hat{e}_z$. The AFM exhibits properties like anti-aligning. This is clear in Fig. 10b where the neighbouring S_y-components are oppositely aligned at $\tilde{t} = 3$. Their amplitudes decrease rapidly and reaches zero much faster than for the FM. We notice that the S_z-components anti-aligns even faster. The reason for why exactly the $z-$components of the spin reaches a non-zero value in equilibrium is due to the anisotropy constant in the Hamiltonian favoring alignments along this particular axis.

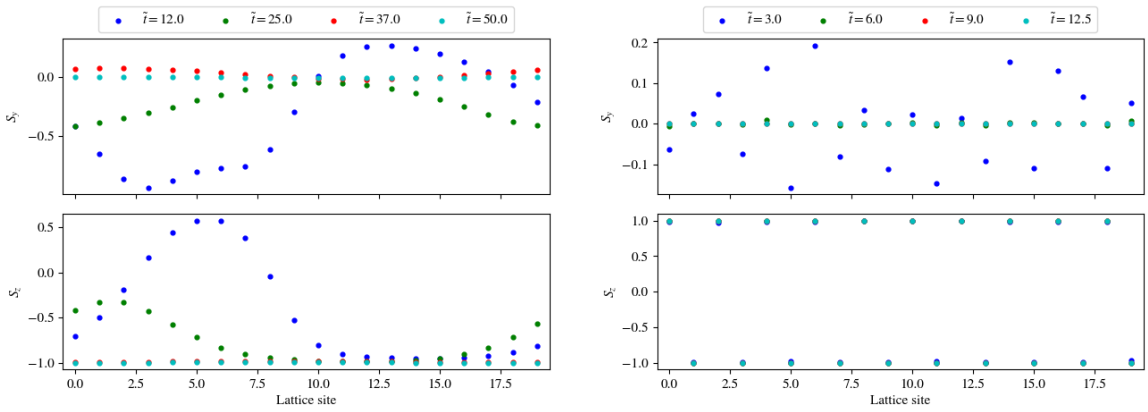

(a) FM, $J > 0$.

(b) AFM, $J < 0$.

Figure 10: Plot of the S_y and S_z components of the spin for each lattice site at different times. The numerical solution solves SCD with $N = 20$, $\alpha = 0.1$ on a grid of resolution $n = 2500$. The spins are initialized randomly, and periodic boundary conditions are utilized.

3.3 Lattice spin

The spins are now placed out on a square lattice of dimensions $N \times N$, yielding a number of N^2 spins. We return to the non-dimensionless form of the LLG equation in order to e.g. set $B = 0$. We then find the expression

$$\vec{F}_j = 2\frac{J}{\mu_s}\sum_{\text{n.n}}\vec{S}_i + 2\frac{d_z}{\mu_s}\vec{S}_{j,z}\hat{e_z} + \vec{B} + \vec{\Gamma}\sqrt{\frac{2\alpha k_b T}{\gamma \mu_s \Delta t}}, \tag{9}$$

which is the used expression for $\vec{F}_j$ in Eq. (2). We set $\mu_s = \mu_B$, and the values for μ_B, γ and k_b are listed in [Eva]. Moreover, $J = 1\text{meV}$, $\alpha = 0.9$, $\Delta t = 1\text{fs}$, $N = 50$, $d_z = 0.1J$ and $\vec{B} = [0, 0, B_0]^T$. We refer to this problem as spin lattice dynamics (SLD), where the used values for the temperature and the magnetic field will vary. We start by verifying that the numerical solution behaves as it should for $T = 0$. We have $J > 0$ so the system is expected to reach the FM ground state once equilibrium is reached. Setting the initial condition to a random configuration, as in f), we compute the magnetization as a function of time. The result is shown in Fig. 11 where $B_0 = 0.5J/\mu_s$ and the solution is computed till $t_{\text{end}} = 20\text{ps}$. The system behaves as expected where it reaches the ordered state quickly.

Task g). We now let $T > 0$ and investigate how the magnetization is altered. The spins are initialized to pointing along the $z-$axis, i.e $S_{j,z} = 1$. We will from here on and on-wards always initialize the spins in such a way. The project description tells us that the temperature dependent average magnetization $M(T)$ determines if the system is in the ordered (ferromagnetic) or disordered (paramagnetic) phase. The average magnetization is computed as the temporal average $M(T) = \langle M(T,t)\rangle_t$ where it is essential that the average is taken over time-steps after the system reaches equilibrium. We denote the equilibrium time as t_{eq}. Letting $B_0 = 0.5J/\mu_s$ and $k_bT/J = 0.05 \implies T = 0\,58\text{K}$ we obtain the magnetization plotted in Fig. 12. The averaged magnetization for this particular temperature is determined to be $M_{\text{ave}} = 0.991 \pm 0.0002$ and is shown in the figure in black and the standard deviation is represented with the dashed lines. The average magnetization is calculated by averaging from $t_{\text{eq}} = 10\text{ps}$ to 20ps. Using a time-step of $\Delta t = 1\text{fs}$, we then average over 10 000 data points. The equilibrium time is determined by looking at the graph and see how $M(T,t)$ stops decreasing, and instead fluctuates around a given value.

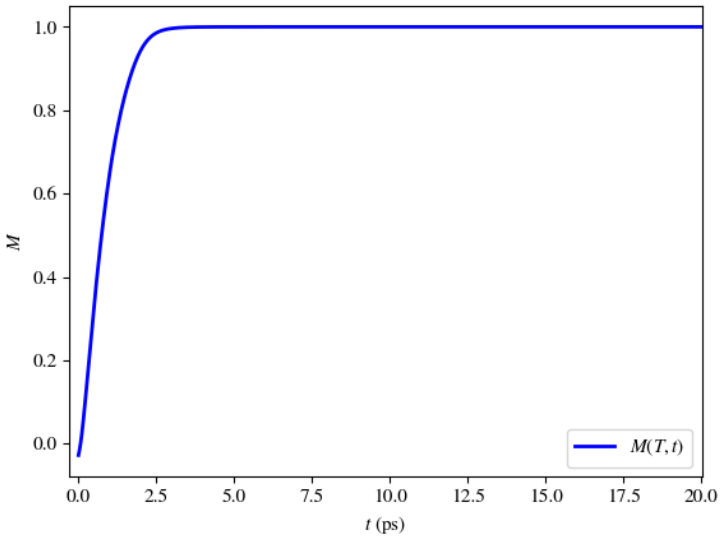

Figure 11: Magnetization as a function when $T = 0$. The numerical solution solves SLD with $B_0 = 0.5J/\mu_s$ and the system starts out in a random configuration.

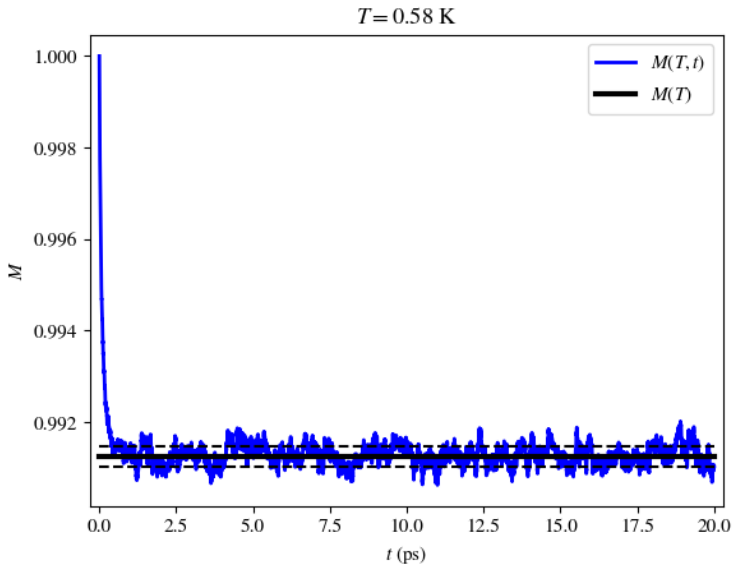

Figure 12: Magnetization of the system as a function of time together with the temporal average taken from $t_{\text{eq}} = 10$ps. In particular, the solution solves SLD with $B_0 = 0.5J/\mu_s$, $k_bT/J = 0.05$ and the initial spins are aligned with the $z-$axis.

Task h). We will here attempt to make a phase-transition plot, i.e. find $M(T)$ as a function of temperature. We proceed in a similar fashion as in g) and use $B_0 = 0.5J/\mu_s$ with the same t_{eq} and Δt. We note that the equilibrium time will in general depend on T, but the chosen value seems to be sufficient after testing for several plots, as Fig. 12, for different temperatures. Proceeding, we set the relative thermal energy, k_bT/J, to range from zero to 23. The magnetic phase diagram, for this particular B_0, is shown in Fig. 13. Once the criterion $M(T) - \sigma < 0$, σ being the standard deviation, is satisfied, do we find the critical temperature T_c. In this case is $T_c = 179.6$K. We note that the colored region in the plot represents the uncertainty, i.e. $\pm\sigma$.

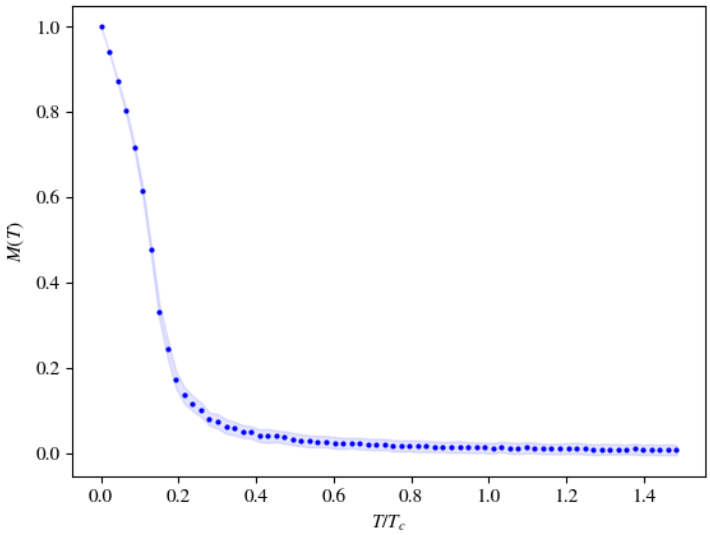

Figure 13: Magnetic phase diagram with $B_0 = 0.5J/\mu_s$. The used parameters are as described in SLD with $t_{\text{eq}} = 10$ps and $t_{\text{end}} = 20$ps. The critical temperature is $T_c = 179.6$K.

Task i). We will now change the magnetic field and find new phase diagrams. In particular, we choose $B_0 = 0.25J/\mu_s$ and $B_0 = 0$. Similar tests as in g) are performed to find the equilibrium time for each magnetic field. The conclusion is that it takes longer time to reach equilibrium when B_0 is reduced. We use $t_{\text{eq}} = 15$ps with $t_{\text{end}} = 25$ps for $B_0 = 0.25J/\mu_s$ and $t_{\text{eq}} = 20$ps with $t_{\text{end}} = 30$ps for $B_0 = 0$. The same parameters in SLD are used otherwise. The results are shown in Fig. 14, where we include the above calculated case. Fig. 14a shows the phase diagrams with a 'normal' temperature axis, while Fig. 14b scales each axis with its own critical temperature. The critical temperatures for the two new magnetic fields are $T_c = 18.56$K and $T_c = 100.2$K for $B = 0$ and $B = 0.25J/\mu_s$ respectively. The phase diagrams for $B_0 > 0$ are continuous, and an increment in B_0 yields a higher critical temperature. This is reasonable since a larger B_0 will push the spins more to align with the $z-$axis, and so it requires more thermal energy to deviate from this position. If we look at the plot with the T/T_c axis can we see that the magnetic field pushes the curve inwards to origin.

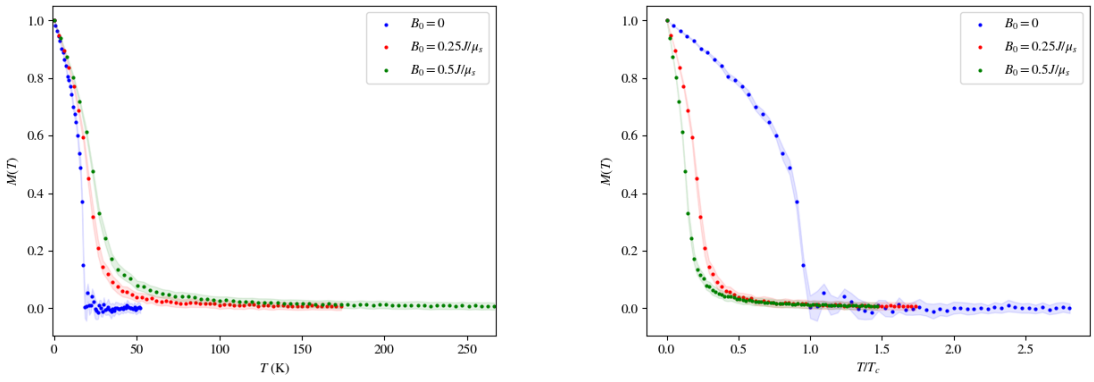

(a) (b)

Figure 14: Phase diagrams for $B_0 = 0.5,\ 0.25,\ 0 \times J/\mu_s$. The used parameters are as in SLD, with $t_{\text{eq}} = 10, 15, 20$ps for each case and we sample data to $t_{\text{end}} = t_{\text{eq}} + 10$ps. The critical temperatures are determined to be $T_c = 179.6,\ 100.2,\ 18.56$K.

We may also test how the phase diagram changes if we remove the anisotropy term in Eq. (9), i.e. set $d_z = 0$. This is done for the two cases where $B_0 = 0$ and $B_0 = 0.5J/\mu_s$, and shown in Fig. 15. The critical temperature decreases when the term is removed. More specifically, for $B_0 > 0$ is the new critical temperature $T_c = 170$K, while for $B_0 = 0$ do we get the same result as earlier. Since the anisotropy term also favours the $z-$axis, can we look at a removal of this term as a decrement in B_0. Thus, when $d_z = 0$ will the effective B_0 decrease and the critical temperature decreases, as discussed in the above paragraph. The project description underlines that the model we are investigating is a semi-classical model. This is clearly shown in Fig. 15a where we have magnetization at low temperatures even though d_z and B_0 is equal to zero. We would not expect such a behaviour from a 2D quantum mechanical model [Sim].

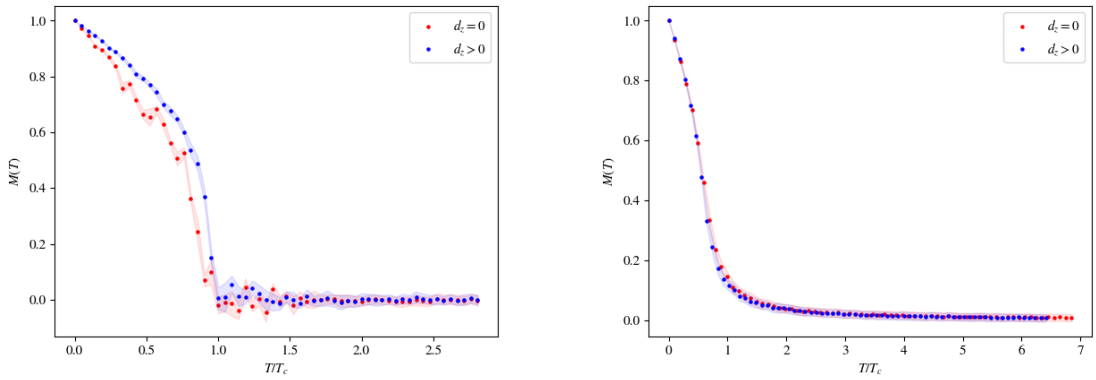

(a) $B_0 = 0$. (b) $B_0 = 0.5J/\mu_s$.

Figure 15: Phase diagrams for $B_0 = 0.5,\ 0 \times J/\mu_s$, with and without the anisotropy term in Eq. (9). We use the parameters listed for SLD, where we use $t_{\text{eq}} = 10,\ 20$ps and run the simulation for each temperature to $t_{\text{end}} = t_{\text{eq}} + 10$ps.

Bibliography

[Eva] Richard Evans. "Atomistic spin simulations of magnetic nanomaterials". In: (). DOI: https://iopscience.iop.org/article/10.1088/0953-8984/26/10/103202/pdf.

[Sim] Ingve Simonsen. *Exam in TFY4235 Computational Physics*. URL: http://web.phys.ntnu.no/~ingves/Teaching/TFY4235/Exam/Exam_tfy4235_2022.pdf.